Appl Water Sci (2013) 3:293–309
DOI 10.1007/s13201-013-0082-5

ORIGINAL ARTICLE

Removal of arsenic(III) and arsenic(V) on chemically modified low-cost adsorbent: batch and column operations

Palas Roy · Naba Kumar Mondal · Shreya Bhattacharya · Biswajit Das · Kousik Das

Received: 19 August 2012 / Accepted: 7 January 2013 / Published online: 3 February 2013

Abstract Batch and column operations were performed utilizing thioglycolated sugarcane carbon (TSCC), a low-cost adsorbent, to remove As(III) and As(V) from aqueous systems. Under optimized batch conditions, the TSCC could remove up to 92.7 and 91.4 % for As(III) and As(V), respectively. An artificial neural network model showed the validity of TSCC as a preferable adsorbent for arsenic [As(III) and As(V)] removal in batch studies. In column operations, removal efficiency increases with increase in influent arsenic concentration and adsorbent dose and decreases with increase in flow rate. At an adsorbent dose of 6.0 g, flow rate 3.0 mL min^{-1}, and initial arsenic concentration 1,500 μg L^{-1}, the arsenic uptake capacity of TSCC for As(III) and As(V) was found to be 85.01 and 83.82 μg g^{-1}, respectively. The Thomas model was used to analyze the column experimental data. Results from the column operations indicated that the adsorption behavior of arsenic [As(III) and As(V)] fits exceptionally well with the Thomas model with high correlation coefficient and very low standard error. Examinations of scanning electron microscopy and FTIR spectroscopy reveal that high arsenic adsorption favors surface complexation on the adsorbent surface.

Keywords Arsenic · Removal · Low-cost adsorbent · Batch · Column

P. Roy · N. K. Mondal (✉) · S. Bhattacharya · B. Das · K. Das
Department of Environmental Science, The University of Burdwan, Burdwan 713104, West Bengal, India
e-mail: nkmenvbu@gmail.com

Introduction

Arsenic's history in applied science has been overshadowed by its notoriety and become synonymous with toxicity (Mohan and Pittman 2007). The existence of arsenic in groundwater, and eventually in drinking water, is a serious environmental and health problem (Ranjan et al. 2009; Biterna et al. 2010) in several developing regions (Haque et al. 2007). High levels of arsenic in drinking waters are now recognized as a worldwide problem associated with 21 countries. The largest population currently at risk is in Bangladesh followed by West Bengal in India (Mohan and Pittman 2007). Today, in West Bengal, the arsenic contamination in groundwater has been detected in 111 blocks in 12 districts of the state (Mondal et al. 2011), affecting more than 1.5 million people (De 2008) of whom 25 % are suffering from arsenical skin lesions. The maximum permissible level of arsenic in drinking water recommended by World Health Organization (WHO) is 10 μg L^{-1} and, in West Bengal, it has been adjusted to 50 μg L^{-1} by the Bureau of Indian Standards (BIS) (Devi et al. 2009). Arsenic concentration in drinking water in West Bengal has been reported to range from 0.05 to 3.6 mg L^{-1} in affected zones (De 2008) in the vicinity of the Ganges Delta in the Bengal Basin (Nag et al. 1996; Awual and Jyo 2009).

In groundwater, arsenic is typically present in one of two oxidation states: arsenite (H_3AsO_3, $H_2AsO_3^-$ or $HAsO_3^{2-}$) and arsenate (H_3AsO_4, $H_2AsO_4^-$, $HAsO_4^{2-}$ or AsO_4^{3-}) (Kumari et al. 2005) of which arsenite [As(III)] is 10 times more toxic than arsenate [As(V)] (Wasiuddin et al. 2002; Amin et al. 2006) due to greater combining affinity with the thiol (–SH) part (Teixeira and Ciminelli 2005) of the protein via soft–soft acid–base interaction (Gregus et al. 2009). However, at the low arsenic

concentrations found in drinking water even before treatment, As(V) is instantly converted on ingestion into As(III), and the toxicity of dissolved arsenic is therefore in practice independent of oxidation state. Bodies such as USEPA, EU and WHO specify only total arsenic for drinking water (Sarkar et al. 2008). In West Bengal, arsenic species in contaminated drinking water were found to be arsenate and arsenite in 1:1 ratio (De 2008). Arsenate is typically present in the mono and divalent anionic forms at neutral pH while arsenite occurs primarily in the groundwater (Amin et al. 2006).

To treat arsenic in water systems, developing cost-effective technologies to remove arsenic from water has drawn great attention in the past 20 years. Several physiochemical techniques, such as adsorption, cation exchange, lime softening, reverse osmosis, coagulation and precipitation have been applied to remove arsenic from aqueous systems. Among these technologies, adsorption is mainly used because it is very simple, cost effective and eco-friendly (Ranjan et al. 2009; Srivastava et al. 2012). The technique is also popular because of the availability of a wide range of adsorbents.

Among all types of conventional and non-conventional adsorbents, commercially available activated carbons have been extensively used for arsenic removal because of their extended surface area, micro/mesoporous structure and significant adsorption capacity. Adsorption of arsenic on a carbon surface is mainly solution pH dependent, and the optimum adsorption of arsenic is achieved at pH 5–6 (Yang et al. 2007).

Although activated carbon is a preferred adsorbent, its widespread use is restricted by its cost (Pan et al. 2009). To decrease the cost, some attempts have been made to develop cheaper but effective adsorbents from a variety of agricultural waste materials (Ranjan et al. 2009). If we consider the surface carbon chemistry, only physically active char carbon prepared from these agricultural waste materials is likely to provide good substitutes for activated carbon. Carbonized sugarcane bagasse, i.e., sugarcane carbon (SCC) is an alternative adsorbent to fulfil such a purpose. Only a few studies on SCC as an adsorbent have been conducted (Amin 2008; Krishnan et al. 2011) and no research has been reported on the improved adsorption of arsenic by SCC.

In this study, therefore, SCC was investigated for adsorption of arsenic. SCC was modified via thioglycolic acid impregnation for improving the adsorption of arsenic, because the arsenic uptake mechanism usually involves unspecific ion exchange reactions (Teixeira and Ciminelli 2005). For instance, positively charged acidic (–SH; –COOH) groups, impregnated in an SCC structure, are potential reactive sites to form adsorptive complexes with negatively charged ions, such as arsenate or arsenite. Thioglycolic acid was also selected as it may lead to a change in the chemistry of SCC (e.g., surface charges).

To determine the performance of a newly prepared adsorbent in adsorption systems, batch and column operations are the two types of laboratory experiments usually applied. Batch operations are usually performed to evaluate the ability of a material to adsorb as well as the adsorption capacity of the material (Sekhula et al. 2012). The data obtained from batch operations are, in most cases, limited to a laboratory scale and thus do not provide data which can be accurately applied in industrial and household systems. Column operations, on the other hand, are necessary to provide data which can be applied for industrial and household purposes (Maji et al. 2007; Ranjan et al. 2009).

Consequently, the following study is designed to: (1) develop a new adsorbent from sugarcane carbon by modification with thioglycolic acid, (2) conduct batch operations to examine arsenic [As(III) and As(V)] adsorption using the new adsorbent, and (3) conduct column studies to investigate the arsenite and arsenate characteristics of thioglycolated SCC (TSCC) for higher concentrations of arsenic under an optimum pH condition of batch examination. An artificial neural network (ANN) model was applied upon batch experimental values to confirm the validity of TSCC as low-cost adsorbent for arsenic removal. The Thomas model was employed to evaluate the column adsorption performance. Scanning electron microscopy (SEM) and FTIR spectroscopy were employed to study surface morphology and functional groups.

Materials and methods

Reagents and apparatus

Chemicals of analytical grade were procured from M/S, Merck India Ltd., and used in the study without further purification. To prepare all reagents and standards, double distilled water was used. All glasswares were cleaned by being soaked in 15 % HNO_3 and rinsed with double distilled water. The pH of the solution was adjusted by adding 0.1 M NaOH or HCl.

Instrumentation

A UV–visible spectrophotometer (Systronics, Vis double beam Spectro 1203) with a 1-cm quartz cell was used for spectrophotometric determination of arsenic [As(III) and As(V)] in solution. For stirring, a magnetic stirrer (TARSONS, Spinot digital model MC02, CAT No. 6040, S. No. 173) was used. pH was measured by a digital pH meter (Model No. Systronic-335). A high precision electrical balance (Model No. Sartorius-312) was used for weighing.

A peristaltic pump (Model No. Mrclab-PP-X-10, Israel) was used to treat arsenic [As(III) and As(V)] solution through the TSCC-packed fixed bed in an up-flow mode at desired flow rates. An adsorbent muffle furnace (PTC1, Paragon made) was used for preparing SCC. Surface morphology of the adsorbent was studied by a Hitachi, S-530 (Make: Eiko Engineering, Ltd., Japan) scanning electron microscope. FTIR (Perkin-Elmer, FTIR, Model-RX1 Spectrometer, USA) analyses were also undertaken for the study of internal binding of arsenic [As(III) and As(V)] by the adsorbent.

Adsorbent preparation

To use thioglycolated sugarcane carbon (TSCC) as an adsorbent, SCC was first prepared by the carbonization of raw sugarcane bagasse that was collected from a sugarcane juice shop, Burdwan town, West Bengal, India. The carbonization by a physical activation method of sugarcane bagasse was essentially the same as described by Amin (2008).

A 100 g portion of the SCC with a monoparticle size of 250 μm was treated with 1,000 mL of 1.0 M thioglycolic acid solution for 24 h at 35 °C in a well-ventilated hood. The mixture was filtered through a filter paper (Whatman No. 41 grade) and washed thoroughly, first with double distilled water, then with methanol and finally with double distilled water until pH 7.0 ± 0.1 was attained, and finally air-dried and stored in a vacuum desiccator for future use (Okieimen and Okundaye 1989; Onwu and Ogah 2010; Srivastava et al. 2012).

Characterization of adsorbent

The surface characteristics of the TSCC were examined by the method of Santamarina et al. (2002). Parameters such as specific surface area (S_{AA}), surface charge density (SCD), specific gravity, bulk density, pore volume, particle density, Hausner ratio, porosity, particle size, moisture content, extent of thiolation, cation exchange capacity (CEC), point of zero charge (pH_{zpc}), pH of slurry and conductance were determined. The specific surface area was determined by the methylene blue absorption test method (Aringhieri et al. 1992). The bulk density was determined as the ratio of the bulk mass of the test sample to its bulk volume. The CEC was determined by the ammonium acetate saturation method (Skinner et al. 2001). The pH_{zpc} was estimated by the method of Mondal (2010). The extent of thiolation was determined by reaction of 0.05 g portions of the TSCC adsorbent with iodine at pH 7.2 ± 0.1, followed by back titration of the unreacted iodine with standard thiosulphate solution (Okieimen and Okundaye 1989; Onwu and Ogah 2010).

Experimental setup

Estimation of arsenic [As(III) and As(V)] was carried out spectrophotometrically by silver diethyl dithiocarbamate (SDDC) method (De 2008; Gupta and Sankararamakrishnan 2010) with precautions to prevent formation of sulfide at the time of arsine generation. The lower detection limit was found to be 2 μg. Each sample was analyzed three times and the results were found reproducible within ±3 % (relative standard deviation) error limit. Calibration was also carried out daily with a freshly prepared arsenic standard, before analysis.

In the batch operation, the effect of different parameters (i.e., pH, contact time, initial concentration of arsenic [As(III) and As(V)], dose of adsorbent, stirring rate and temperature) on adsorption of arsenic [As(III) and As(V)] was studied. The 100 mL solutions of As(III) (sodium arsenite; $NaAsO_2$) and As(V) (sodium hydrogen arsenate; $Na_2HAsO_4{\cdot}7H_2O$) were taken in separate Erlenmeyer flasks. After pH adjustments, a known quantity of dried TSCC adsorbent was added and the arsenic [As(III) and As(V)] bearing suspensions were kept under magnetic stirring until the equilibrium conditions were reached. After shaking, the suspension was allowed to settle down and filtered using a Whatman 42 grade filter paper. The filtrate was collected and subjected for arsenic estimation using the SDDC method. The arsenic concentrations before and after adsorption were recorded, and then the percent arsenic adsorption (removal) by the adsorbent was computed using (Kumari et al. 2005; Amin et al. 2006; Das and Mondal 2011; Srivastava et al. 2012) the equation.

$$\text{Percent adsorption (removal)} = [(C_i - C_e)/C_i] \times 100$$

where C_i and C_e are the initial and final concentration of arsenic [As(III) and As(V)] in the solution.

The arsenic uptake loading capacity ($q_e = \mu g\ g^{-1}$) of TSCC for each concentration of arsenic [As(III) and As(V)] at equilibrium was also determined by using the following equation:

$$q_e = \frac{(C_i - C_e)}{M} \times V$$

where V is the volume of solution (L) and M is the mass of the adsorbent (g) used (Gupta and Sankararamakrishnan 2010; Das and Mondal 2011; Krishnan et al. 2011).

Fixed bed column operations were conducted using borosilicate glass columns of 3 cm internal diameter and 50 cm length. The column was packed with different amounts of TSCC, in order to achieve different bed heights, between two supporting layers of 1 cm of glass wool in order to prevent the floating of adsorbent from the outlet. A schematic diagram of the column is shown in Fig. 1.

The column studies were conducted to evaluate the effects of various parameters, viz., initial arsenic [As(III) and As(V)] concentration, the flow rate, and the bed height

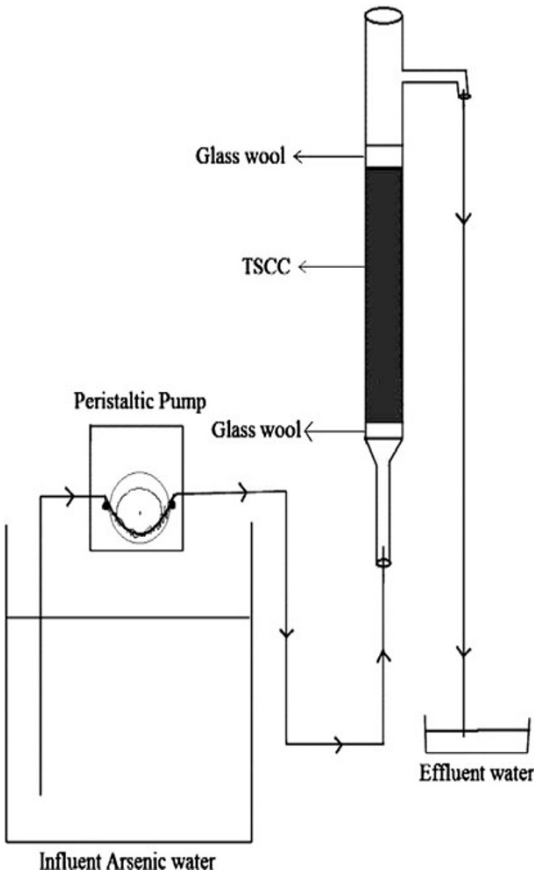

Fig. 1 Schematic diagram of the experimental setup for column operation

(adsorbent dose). Arsenic [As(III) and As(V)] solution having the desired initial concentration was adjusted to the optimum batch pH for the maximum uptake of arsenic, and pumped through the column at the desired flow rate through the bed in an up-flow mode. The flow rates were chosen to have sufficient amount of effluent per 30 min for the practical purpose of analyzing arsenic [As(III) and As(V)] concentration. Operation of the column was stopped when the effluent concentration exceeded a value of 99 % of the initial arsenic [As(III) and As(V)] concentration. All of the experiments were carried out in triplicate at room temperature (30 °C), and the mean values were taken. In this column study, the Thomas model (Thomas 1944) and error analysis have been performed for evaluation of efficiency and applicability of the operations.

Results and discussion

Characterization of TSCC

The TSCC was found to be stable in water, dilute acids and bases. The adsorbent behaves as neutral at pH zero charge. Adsorption of cations is favored at $pH > pH_{zpc}$, while the adsorption of anions is favored at $pH < pH_{zpc}$ (Mondal 2010). The point of zero charge is 4.68 irrespective of difference in concentration of the HNO_3 used. The physico-chemical properties of TSCC are summarized in Table 1.

The SEM photomicrographs (25 kV; 20 μm) of SCC and TSCC are given at 2,000 magnification in Figs. 2 and 3, respectively. Figure 2 clearly shows the presence of fibrous, rough and irregular surface morphology of SCC. Meanwhile, the micrograph shown in Fig. 3 depicts the significant deformation in the structural organization of the fibrous SCC surface to flat shape with higher fragmentation

Table 1 Physico-chemical characteristics of TSCC

Analysis	Value
pH_{slurry}	4.16 ± 0.21
pH_{zpc}	4.68 ± 0.13
Specific gravity	0.274 ± 0.01
Moisture content (%)	13.11 ± 0.23
Bulk density (g cm^{-3})	0.386 ± 0.01
Particle density (g cm^{-3})	1.47 ± 0.52
Hausner ratio	0.25 ± 0.01
$Conductivity_{slurry}$ (μS cm^{-1})	0.93 ± 0.09
Porosity (%)	74.97 ± 3.08
Particle size (μm)	250 ± 4.81
Pore volume (cm^3 g^{-1})	2.307 ± 0.17
Specific surface area (m^2 g^{-1})	5.69 (±1.41) × 10^3
Extent of thiolation (%)	33.31 ± 0.02
Cation exchange capacity (meq g^{-1})	1.35 (±0.21) × 10^3
Surface charge density (meq m^{-2})	0.24 ± 0.01

(±Standard error of mean)

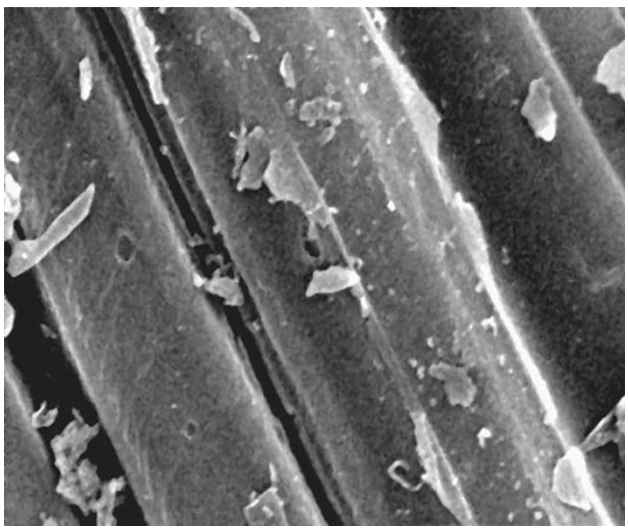

Fig. 2 SEM image of SCC

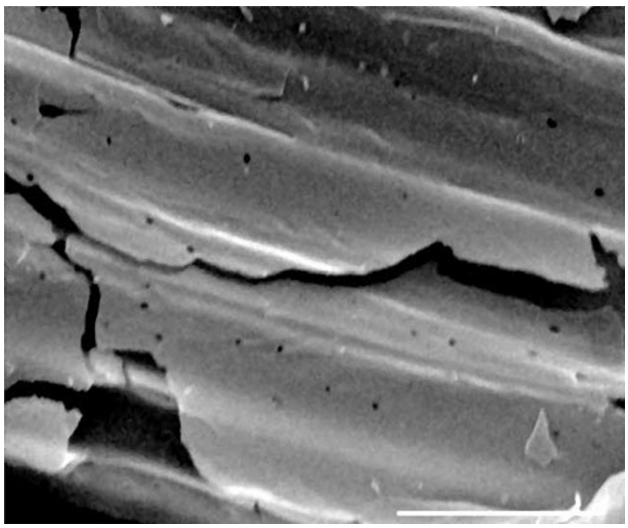

Fig. 3 SEM image of TSCC

and roughness. This change in surface texture is favorable for high adsorption capacity in the adsorption process.

The FTIR spectra of SCC and TSCC, presenting the plot of percentage transmission versus wave number (Fig. 4), have been measured to analyze the different types of functional groups. In Fig. 4, a number of absorption peaks for SCC observed at 3,424, 2,927, 2,858, 1,576, 1,420, 1,260 and 781 cm^{-1} represent N–H stretching of primary aromatic amine, $>CH_2$ asymmetrical stretching, symmetrical stretching $>CH_2$ group, skeletal vibration of aromatic C=C, deformational vibration of =C–H of alkenes, C–N stretching of aromatic primary amine and –C–H out of plane deformation of aromatic compounds, respectively (Kemp 1996; Furniss et al. 2005; Ghosh 2006). After treatment with thioglycolic acid, a significant decrease of these bands was noted in the spectrum of TSCC along with two new peaks at 1,702 and 1,094 cm^{-1} indicating C=O stretching of saturated acid (Furniss et al. 2005; Ghosh 2006) and C–S axial stretching (Papaleo et al. 1996) of thioglycolic acid. Moreover, the absence of the characteristic frequency at 1,420 cm^{-1} also shows the existence of structural disorder which has been explained as a result of chemical interaction between alkene groups of SSC and thioglycolic acid at its surface.

Batch operation

Effect of initial arsenic concentration

The adsorption behavior of two states of arsenic [As(III) and As(V)] species was studied in the arsenic concentration range 50–500 μg L^{-1} at pH 6.0. In general, the removal percentage of As(III) and As(V) on TSCC adsorbent initially increased with the increasing initial concentration of arsenic reaching the optimum level of 86.3 and 85.6 %, respectively, at 100 μg L^{-1} arsenic concentration. Thereafter, the percentage of removal showed little decrease (Figs. 5, 6). But the actual amount of arsenic adsorbed per unit mass of adsorbent increased with increasing initial concentration in the test solution. This increase was due to decrease in resistance to the uptake of solute from solution with increase in arsenic concentration (Nollet et al. 2003; Bhaumik et al. 2011; Suresh et al. 2012).

Effect of adsorbent dose

While observing the influence of the dry weight of TSCC mass on the removal capacity at pH 6.0, it was found that the removal capacity of both the arsenic [As(III) and As(V)] species increased (Figs. 7, 8) with increased adsorbent doses (0.05–0.25 g). No significant increment in the removal tendency was noted on further increasing the

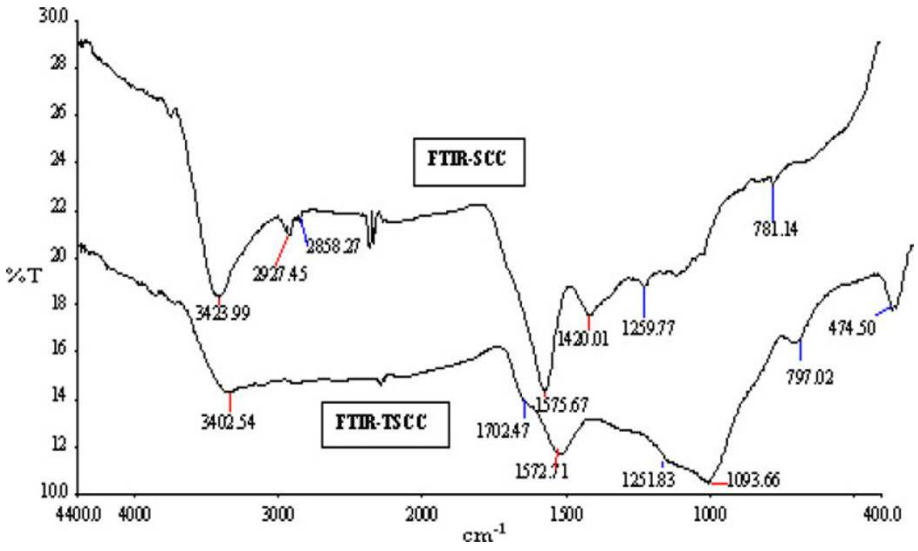

Fig. 4 FTIR spectra of SCC and TSCC

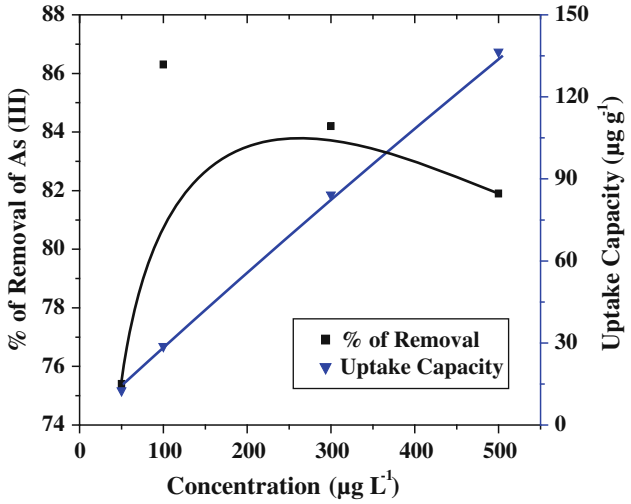

Fig. 5 Effect of initial arsenic concentration on the adsorption of As(III) by TSCC. Dose = 0.15 g, contact time = 20 min, pH = 6, temperature = 25 °C, stirring rate = 50 rpm

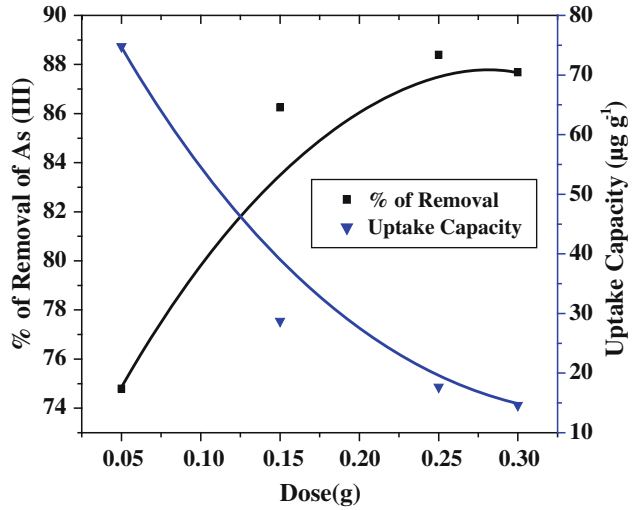

Fig. 7 Effect of adsorbent dose on the adsorption of As(III) by TSCC. Initial arsenic concentration = 100 µg L^{-1}, contact time = 20 min, pH = 6, temperature = 25 °C, stirring rate = 50 rpm

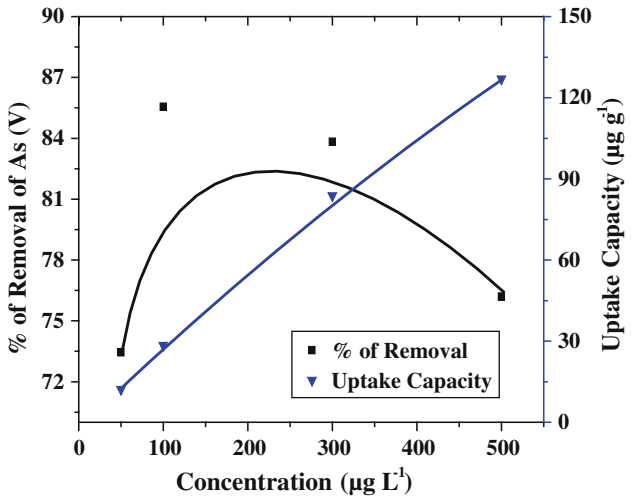

Fig. 6 Effect of metal concentration on the adsorption of As(V) by TSCC. Dose = 0.15 g, contact time = 20 min, pH = 6, temperature = 25 °C, stirring rate = 50 rpm

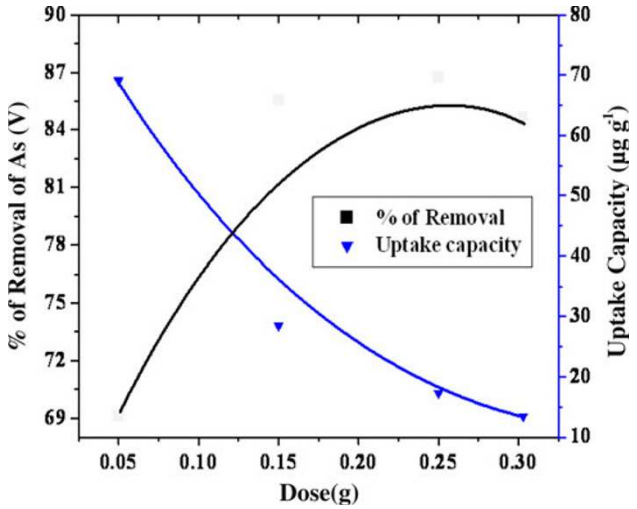

Fig. 8 Effect of adsorbent dose on the adsorption of As(V) by TSCC. Initial arsenic concentration = 100 µg L^{-1}, contact time = 20 min, pH = 6, temperature = 25 °C, stirring rate = 50 rpm

mass dosages from 0.25 g onwards. Increasing the removal tendency with adsorbent dose can be attributed to increase in adsorbent surface area and the availability of more active binding sites (Lewinsky 2007; Das and Mondal 2011).

Effect of contact time

The effect of contact time on the adsorption of both the arsenic [As(III) and As(V)] species on TSCC adsorbent was studied in the duration of 10–40 min at pH 6.0 and 2.5 g dose. The percentage removal of arsenic ions as a function of time suggested a biphasic pattern (Kumari et al. 2005) on the TSCC surface with a rapid initial uptake up to 30 min, which gradually reached equilibrium after a period of 30 min (Figs. 9, 10). Thereafter, no significant increase in adsorption percentage was found. The fast adsorption rate at the initial stage may be explained by increased availability in the number of active binding sites on the adsorbent surface. After a lapse of time, the remaining vacant surface sites are difficult to occupy because of repulsive forces between the solute molecules on the solid and bulk phases (Rajesh Kannan et al. 2010; Das and Mondal 2011).

Effect of pH

Figures 11 and 12 represent the percentage removal (or uptake capacity) as a function of the pH at optimum concentration (100 µg L^{-1}) of As(III) and As(V), respectively. The

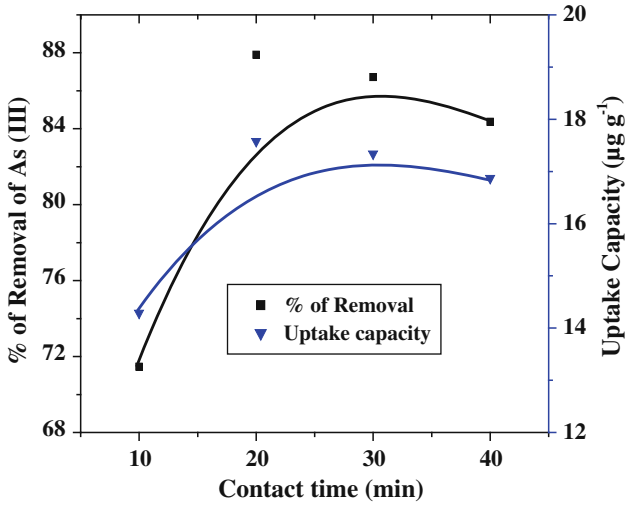

Fig. 9 Effect of contact time on the adsorption of As(III) by TSCC. Initial arsenic concentration = 100 μg L^{-1}, dose = 0.25 g, pH = 6, temperature = 25 °C, stirring rate = 50 rpm

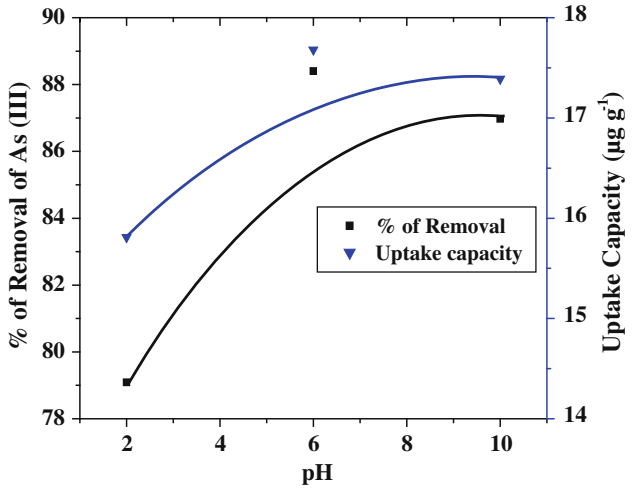

Fig. 11 Effect of pH on the adsorption of As(III) by TSCC. Initial arsenic concentration = 100 μg L^{-1}, dose = 0.25 g, contact time = 20 min, temperature = 25 °C, stirring rate = 50 rpm

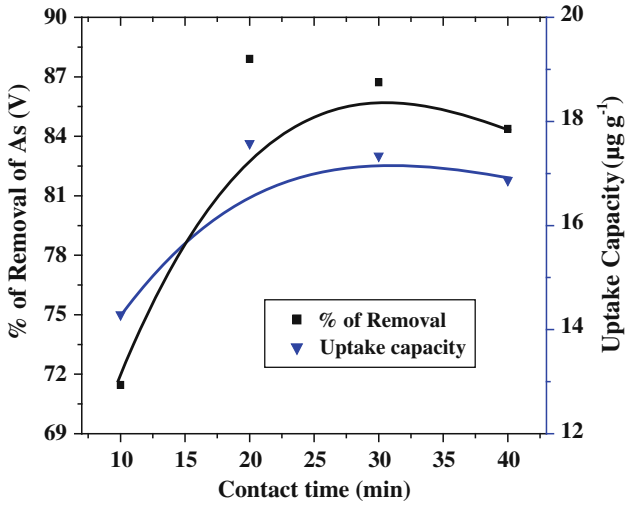

Fig. 10 Effect of contact time on the adsorption of As(V) by TSCC. Initial arsenic concentration = 100 μg L^{-1}, dose = 0.25 g, pH = 6, temperature = 25 °C, stirring rate = 50 rpm

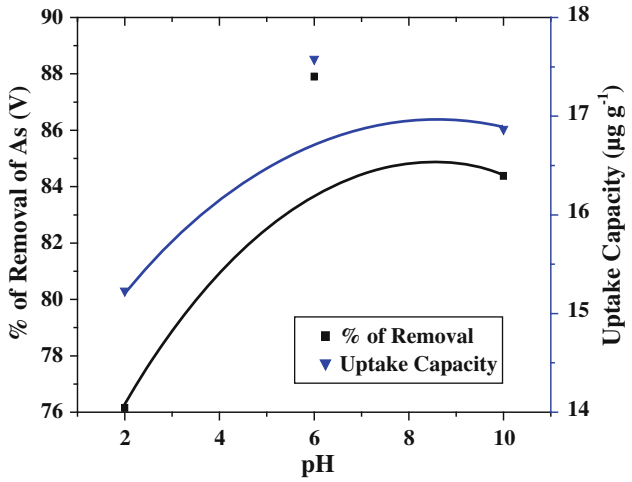

Fig. 12 Effect of pH on the adsorption of As(V) by TSCC. Initial arsenic concentration = 100 μg L^{-1}, dose = 0.25 g, contact time = 20 min, temperature = 25 °C, stirring rate = 50 rpm

optimum removal 88.4 % (17.7 μg g^{-1}) and 87.9 % (17.6 μg g^{-1}) were obtained at the pH of 6.0 by the TSCC adsorption of the both As(III) and As(V) species, respectively. This is attributed to the surface complexation on the adsorbent surface being highly favored at this pH (Yang et al. 2007; Hao et al. 2009). At the moment of complexation at pH 6.0, arsenite is present as H_3AsO_3 ($pKa_1 \sim 9.2$), whereas for arsenate $H_2AsO_4^-$ ($pKa_1 \sim 6.7$) is the predominant species. The probable mechanism for the surface complexation reaction is shown in Fig. 13. Under the optimized pH condition, each As(III) ion binds to three sulfur atoms on the TSCC surface, and three water molecules are released. Whereas As(V) binds with two oxygen atoms of carboxylate groups (Schmidt et al. 2008; Tiwari et al. 2008) and releases two water molecules. The choice of bindings is in full accord with the soft–hard acid–base principle. At high pH, less surface complexes were formed due to the electrostatic repulsion between the ionized species $H_2AsO_3^-$ or $H_2AsO_4^-$ and thioglycolates.

Effect of temperature

The influence of temperature on the removal of arsenic [As(III) and As(V)] by TSCC was measured at different temperatures ranging from 25 to 45 °C. Figures display the percent removal for both As(V) and As(III) increased with temperature, from 87.9 to 90.2 % for As(V) (Fig. 15) and from 88.4 to 92.0 % for As(III) (Fig. 14) when temperature

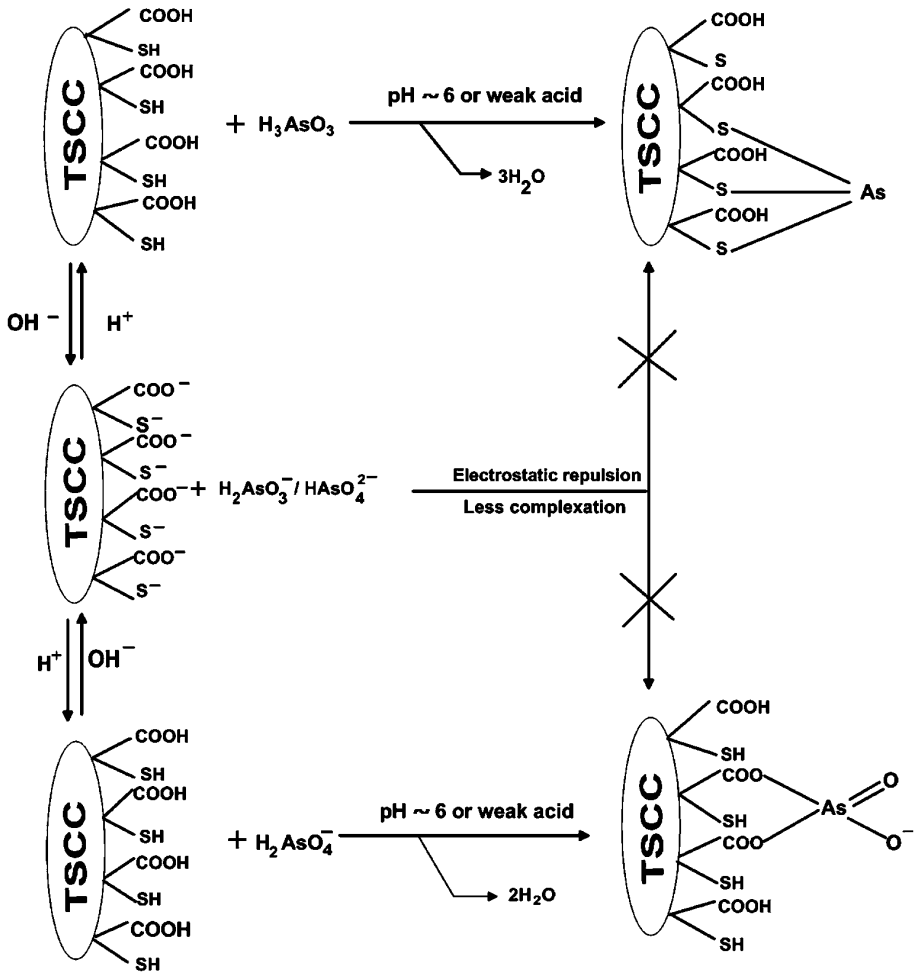

Fig. 13 Schematic representation of the arsenic [As(III) and As(V)] adsorption mechanism and the effect of pH

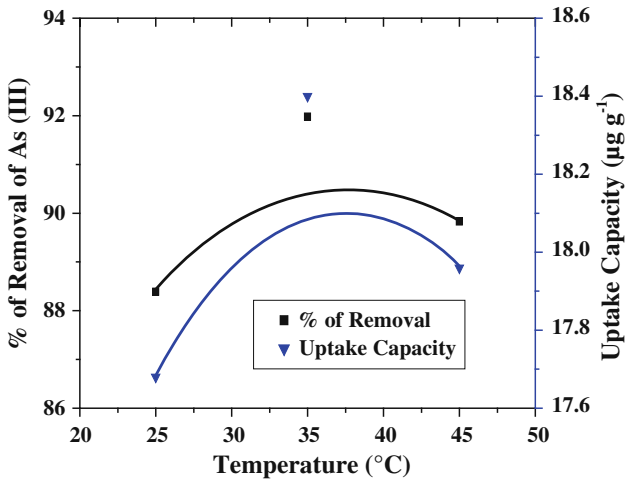

Fig. 14 Effect of temperature on the adsorption of As(III) by TSCC. Initial arsenic concentration = 100 µg L^{-1}, dose = 0.25 g, contact time = 20 min, pH = 6, stirring rate = 50 rpm

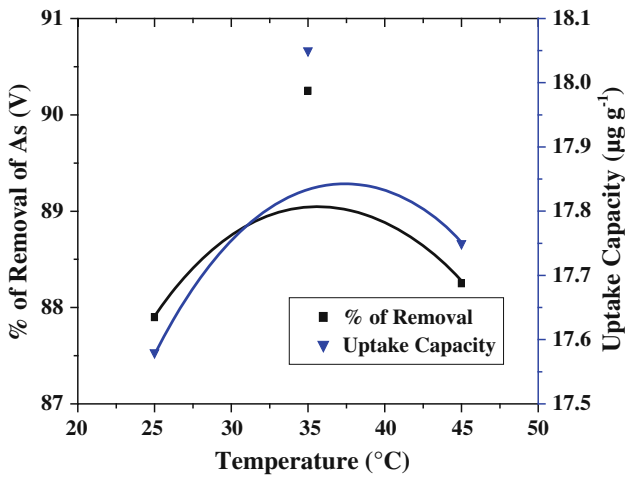

Fig. 15 Effect of temperature on the adsorption of As(V) by TSCC. Initial arsenic concentration = 100 µg L^{-1}, dose = 0.25 g, contact time = 20 min, pH = 6, stirring rate = 50 rpm

was increased from 25 to 35 °C and removal almost reached equilibrium at 35 °C and then decreased. This explains why at very high temperature TSCC loses its adsorbent power through denaturation (Rajesh Kannan et al. 2010).

Effect of stirring rate

The effect of different stirring rate was observed by varying speeds from 50 to 200 rpm, and it appears that the

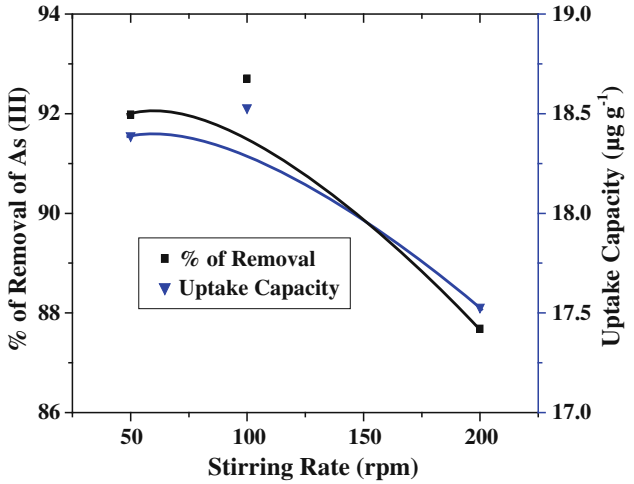

Fig. 16 Effect of stirring rate on the adsorption of As(III) by TSCC. Initial arsenic concentration = 100 μg L^{-1}, dose = 0.25 g, contact time = 20 min, pH = 6, temperature = 35 °C

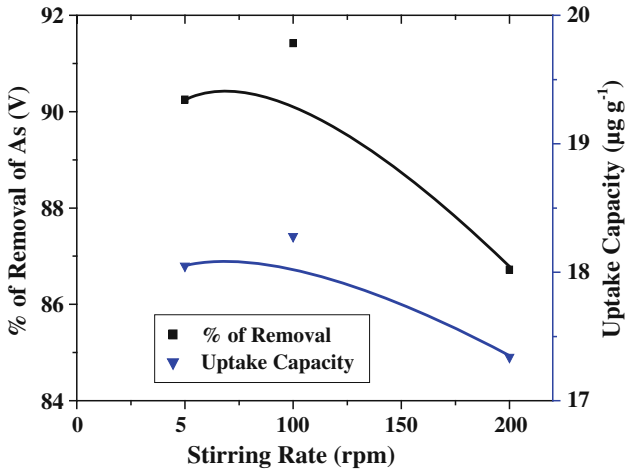

Fig. 17 Effect of stirring rate on the adsorption of As(V) by TSCC. Initial arsenic concentration = 100 μg L^{-1}, dose = 0.25 g, contact time = 20 min, pH = 6, temperature = 35 °C

percentage of arsenic [As(III) and As(V)] removal increased with the decrease in stirring rate. An increasing stirring rate did not give appropriate time for adsorbate and adsorbent surfaces to interact with each other and also resulted in detachment of loosely bound ions. At 100 rpm, maximum removal of 92.7 and 91.4 % occurred for As(III) and As(V), respectively; but below 100 rpm, there was no significant increase in the rate of removal. This is because all the binding sites have been utilized and no binding sites were available for further adsorption (Kanwal et al. 2012) (Figs. 16, 17).

Artificial neural network (ANN) modeling

In the last decade, ANN modeling has been successfully applied for estimating and predicting adsorption properties that are function of many variables and parameters. ANN is a mathematical or computational model for processing of information based on the connectionist approach. This model has the ability to learn from existing data and adopt to map a set of input parameters into a set of output parameters, without knowing the intricate relationship among them. ANN can be trained to identify patterns and extract trends in imprecise and complicated non-linear data (Giri et al. 2011). As adsorption is a complex non-linear process, neural network are found suitable for prediction of arsenic adsorption (removal) efficiency. Neural Network Toolbox Neuro Solution 5® mathematical software was used to evaluate arsenic [As(III) and As(V)] removal efficiency. Figure 18 shows the ANN model used in this study.

The input vectors, 16 sets of experimental data for each arsenic species contain pH, initial concentration, adsorbent dosage, contact time, stirring rate and temperature. There is just one neuron in the output layer in each case which is the amount of removal. The standardized back-propagation algorithm was used for the training of the input data. Figure 19 shows the plot of amount of removal predicted by ANN versus amount of removal obtained from experiments, during the training process. The slope of the line (0.928; 0.925) and amount R^2 values (0.958; 0.987) show good training of the network.

Column operation

Effect of adsorbent dose

Breakthrough curves for adsorption of arsenic [As(III) and As(V)] at optimum batch pH onto TSCC at various adsorbent doses by fixing influent arsenic concentration (1,000 μg L^{-1}) and flow rate (5.0 mL min^{-1}) are shown in Fig. 20. The various amounts of TSCC used were 2.0, 4.0, and 6.0 g for the columns to produce bed heights of 11.3, 20.9, and 32.1 cm, respectively (Table 2). From Fig. 20, it was also observed that the removal efficiency was increased with the increase in adsorbent dose for both As(III) and As(V). As adsorbent dose increases, bed height increases, arsenic has more time to contact with TSCC which resulted in higher removal efficiency of arsenic in the column. It was the increase in adsorbent doses in larger beds which provided a greater number of adsorption sites for arsenic with increase in the surface area of TSCC (Han et al. 2007; Ranjan et al. 2009).

Effect of flow rate

The effect of flow rate on arsenic [As(III) and As(V)] adsorption by TSCC was studied by varying the flow rate from 3.0 to 7.0 mL min^{-1} and keeping the initial arsenic concentration (1,000 μg L^{-1}), adsorbent dose (6.0 g) and

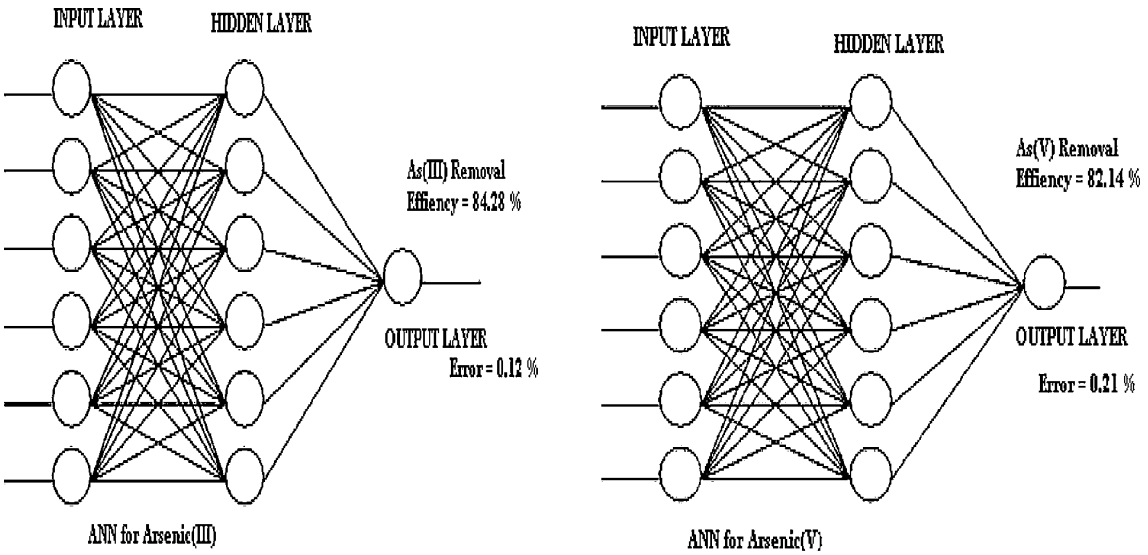

Fig. 18 Neural network architecture of As(III) and As(V)

Fig. 19 Comparison of experimental data and the simulation results in the training step of batch operations

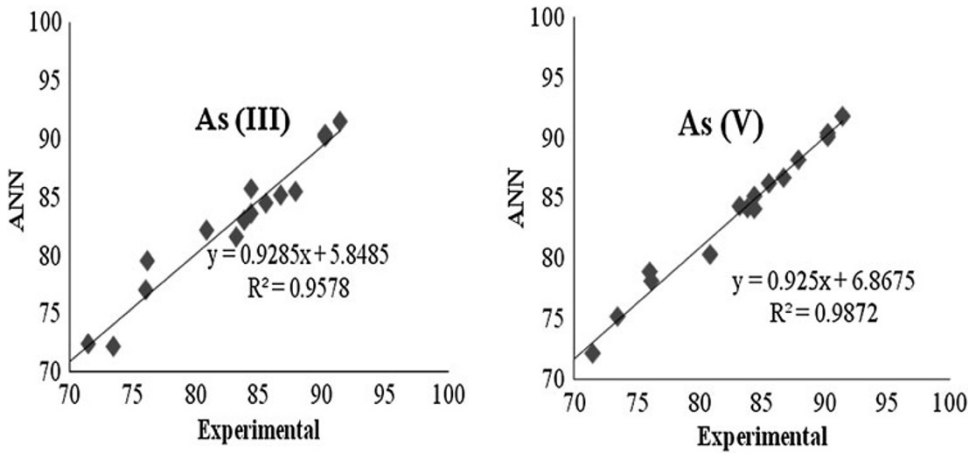

Fig. 20 Breakthrough curves for arsenic adsorption at different adsorbent doses (flow rate = 5.0 mL min^{-1}; initial arsenic concentration = 1,000 μg L^{-1}; pH = 6)

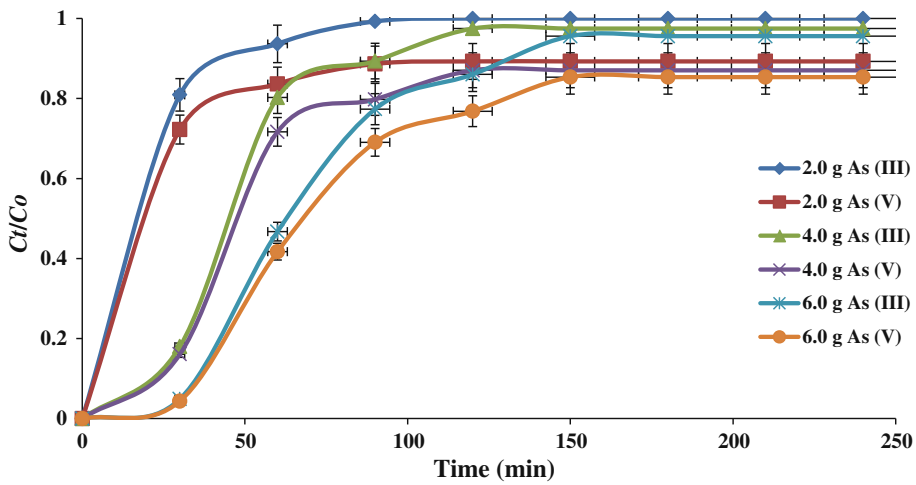

pH constant. The breakthrough curves are shown in Fig. 21. It was found that the adsorption capacity decreased as the flow rate increased (Table 2). The phenomenon can be explained on the basis of insufficient residence time of the solute in the column (Gupta and Sankararamakrishnan 2010; Nidheesh et al. 2012). This insufficient time

Table 2 Modeling of column operation results onto TSCC column

Process parameters	Experimental q_0 for As(III)	Thomas model results for As(III)				Experimental q_0 for As(V)	Thomas model results for As(V)			
	q_{0expt} (μg g^{-1})	k_{Th} (mL min^{-1} μg^{-1})	q_0 (μg g^{-1})	R^2	SE	q_{0expt} (μg g^{-1})	k_{Th} (mL min^{-1} μg^{-1})	q_0 (μg g^{-1})	R^2	SE
Adsorbent dose (g) [Bed height (cm)]										
2.0 [11.3]	48.25	0.081 ± 0.005	49.55 ± 0.62	0.944	0.330	47.34	0.079 ± 0.007	48.86 ± 0.58	0.982	0.184
4.0 [20.9]	58.45	0.054 ± 0.003	61.06 ± 0.78	0.934	0.358	58.27	0.053 ± 0.003	60.21 ± 0.72	0.971	0.239
6.0 [32.1]	61.45	0.047 ± 0.002	64.20 ± 0.82	0.926	0.378	60.75	0.045 ± 0.002	63.30 ± 0.88	0.945	0.327
Flow rate (mL min^{-1})										
3.0	70.09	0.106 ± 0.008	72.63 ± 0.47	0.914	0.406	68.95	0.107 ± 0.009	71.61 ± 0.64	0.918	0.396
5.0	61.60	0.047 ± 0.003	64.20 ± 0.67	0.926	0.378	61.01	0.047 ± 0.003	63.30 ± 0.62	0.945	0.327
7.0	23.78	0.035 ± 0.001	25.31 ± 0.43	0.976	0.216	23.61	0.035 ± 0.001	24.94 ± 0.34	0.981	0.195
Initial concentration (μg L^{-1})										
500	52.35	0.142 ± 0.013	55.01 ± 0.54	0.910	0.415	51.49	0.144 ± 0.017	54.24 ± 0.66	0.912	0.410
1,000	69.41	0.106 ± 0.011	72.63 ± 0.82	0.914	0.406	69.11	0.107 ± 0.010	71.61 ± 0.48	0.918	0.396
1,500	82.27	0.027 ± 0.003	85.01 ± 0.93	0.935	0.355	81.83	0.026 ± 0.003	83.82 ± 0.82	0.973	0.230

(±Standard error of mean)

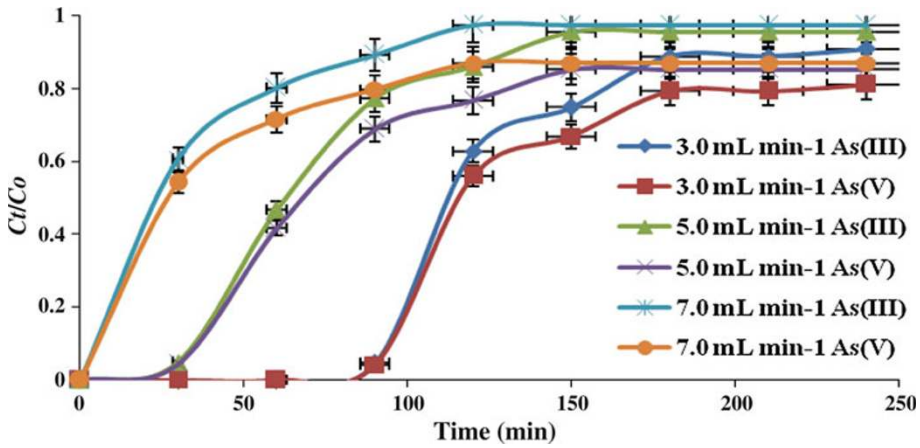

Fig. 21 Breakthrough curve for arsenic adsorption at different flow rates (adsorbent dose = 6.0 g; initial arsenic concentration = 1,000 μg L^{-1}; pH = 6)

decreases the bonding capacity of the arsenic ions onto –SH and –COOH groups present in the adsorbent surface.

Effect of initial arsenic concentration

The effect of the initial arsenic concentration (500, 1,000, and 1,500 μg L^{-1} arsenic) at a constant adsorbent dose of 6.0 g, flow rate of 3.0 mL min^{-1} and pH of 6 is shown in Fig. 22. The figure showed that the adsorption efficiency of TSCC decreased on gradual increase of influent arsenic concentration. This is due to shortening of the mass transfer zone. At higher concentrations, more adsorption sites were covered which saturated the bed more quickly and hence decreased the breakthrough time (Gupta 2008; Ranjan et al. 2009). The experimental and predicted (model) uptake capacity (q_{0expt} and q_0) were also found to increase with the increase in the initial arsenic concentration (Table 2). The reason is that the driving force for adsorption is the concentration difference between the solute on the sorbent and the solute in the solution (Han et al. 2007; Ranjan et al. 2009).

As, the maximum uptake capacity (predicted) of 85.01 and 83.82 μg g^{-1} for As(III) and As(V), respectively, was observed at an adsorbent dose of 6.0 g, flow rate 3.0 mL min^{-1}, and initial arsenic concentration 1,500 μg L^{-1} (Table 2); hence two independent column operations were conducted at this similar conditions to find the amount of retained arsenic in the adsorbent column. With respect to 6.0 g adsorbent dose, the highest arsenic retained amounts for predicted and experimental conditions are shown in Fig. 23. The good agreement between the predicted and experimental values suggests the validity of the column operations for the removal of both As(III) and As(V) by TSCC.

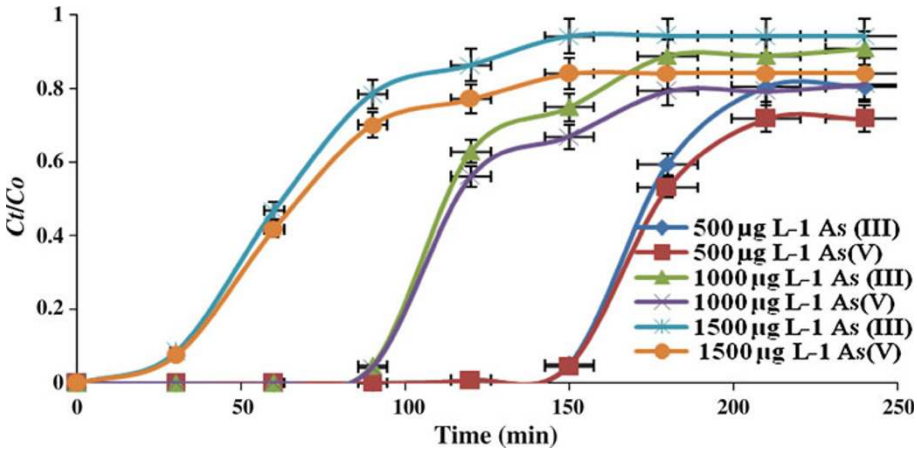

Fig. 22 Breakthrough curve for arsenic adsorption at different initial arsenic concentration (adsorbent dose = 6.0 g; flow rate of = 3.0 mL min^{-1}; pH = 6)

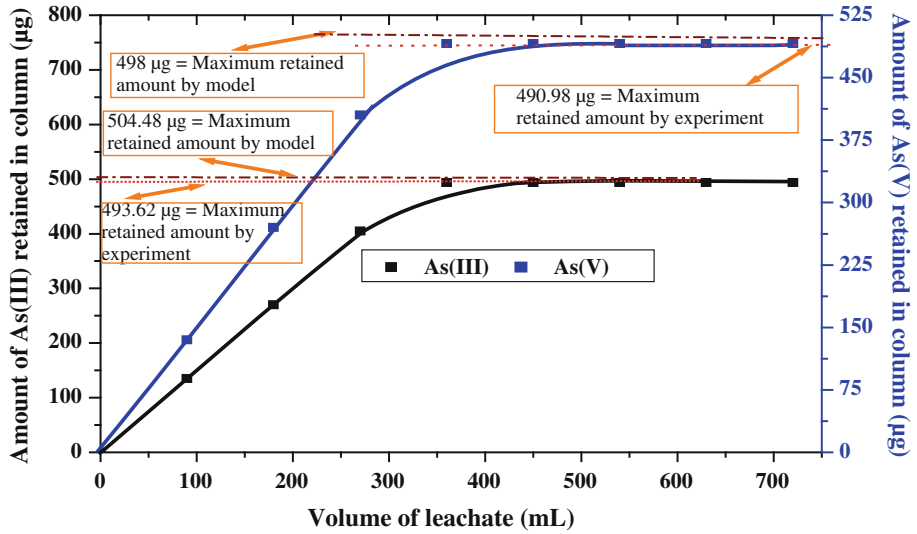

Fig. 23 Column operations for arsenic adsorption at initial arsenic concentration = 1,500 µg L^{-1}; adsorbent dose = 6.0 g; flow rate of = 3.0 mL min^{-1}; pH = 6

The Thomas model

The Thomas kinetic model (Thomas 1944) is one of the most general and widely used methods in fix bed column studies (Chiavola et al. 2012). This column performance theory is developed to calculate the maximum solid phase concentration of the solute on an adsorbent and the adsorption rate constant for continuous adsorption process in column studies (Malkoc and Nuhoglu 2006; Han et al. 2007). The linearized form of the Thomas model for an adsorption column is as follows:

$$Q \times \ln\left(\frac{C_0}{C_t} - 1\right) = (k_{\mathrm{Th}} \times q_0 \times M) - (k_{\mathrm{Th}} \times C_0 \times V_{\mathrm{eff}})$$

where k_{Th} is the Thomas rate constant (mL min^{-1} μg^{-1}), q_0 the equilibrium metal ion uptake per gram of the adsorbent (µg g^{-1}), M the amount of adsorbent in the column (g), V_{eff} the effluent volume (mL) at a given flow rate, C_0 the influent concentration (µg L^{-1}), C_t the effluent concentration (µg L^{-1}) and Q the volumetric flow rate (mL min^{-1}). The value of C_0/C_t is the ratio of effluent and influent concentrations. The adsorption capacity of the column q_0 and kinetic coefficient k_{Th} can be determined from the plot of $[(C_0/C_t) - 1]$ against V_{eff} at a given flow rate.

Error analysis

For nonlinear fitting of kinetic data, the standard error (SE) analysis is used to evaluate the applicability of the model. The SE of the estimate is given as (Han et al. 2007):

$$\mathrm{SE} = \sqrt{\sum \frac{(Q_{\mathrm{e}} - Q_{\mathrm{c}})^2}{N}}$$

where Q_{e} and Q_{c} are the experiment and model calculation values, respectively; N is the number of the experimental points. For the confirmation of the best fit for the adsorption system, it is necessary to analyze the data using SE by combining the values of determined correlation coefficient (R^2).

The Thomas model was applied to the experimental data with respect to influent concentration of arsenic [As(III) and As(V)], flow rate and adsorbent dose. Thomas model parameters of q_0 and k_{Th} were determined on each set of data by regression analysis. The R^2 and SE were also obtained using regression analysis. The results are listed in Table 2.

Column operation results (Table 2) show that rate constant decreases with increase in influent concentration, decreases with increase in adsorbent dose and increase in flow rate. In general, equilibrium uptake capacity decreases on increasing flow rate and increases on increasing influent concentration of both As(III) and As(V). These findings could be attributed to the higher driving force of the higher inlet concentration (Han et al. 2007) of arsenic. The results also indicate that the adsorption behavior of arsenic [As(III) and As(V)] fits exceptionally well with the Thomas model with high correlation coefficient and very low SE.

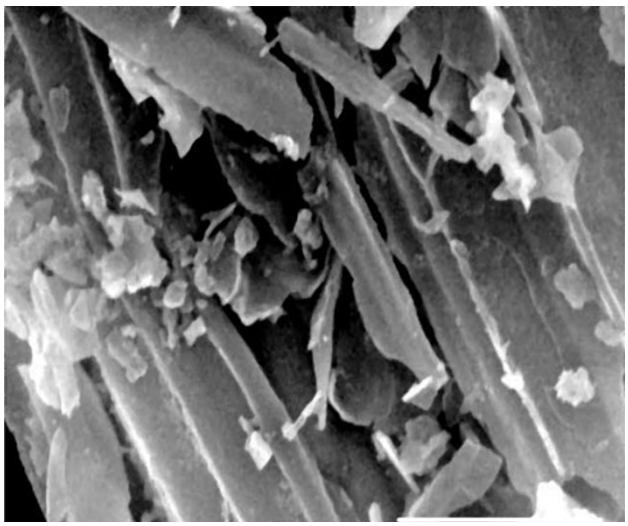

Fig. 24 SEM image of TSCC after treatment of As(III) in batch operation

SEM study

The SEM images of TSCC for both batch and column operations, after passing of arsenic [As(III) and As(V)] solution through TSCC are shown in Figs. 24, 25, 26 and 27. All figures clearly show the changes on the surface of the TSCC indicating the adsorption to be a surface phenomenon. The significant deformation in the structural organization of the TSCC, after passing arsenic solution, attributed toward the high adsorption of arsenic on the adsorbent surface. This adsorption behavior is further supported by the FTIR study.

FTIR study

FTIR spectroscopy was carried out for studying the interaction between adsorbate [As(III) and As(V)] and the active groups on the surface of the adsorbent and the changing of the spectrum attributed to the adsorption reaction. After treatment of arsenic solution through TSCC, the resulting FTIR spectra of batch and column operations gave similar results for each arsenic [As(III) and As(V)] species. Thus only two spectra are shown in Fig. 28.

The absorption peaks at 3,424–3,425, 2,930, 1,718, 1,578, 1,420 and 781 cm^{-1} represent above-mentioned N–H stretching of primary aromatic amine, $>CH_2$

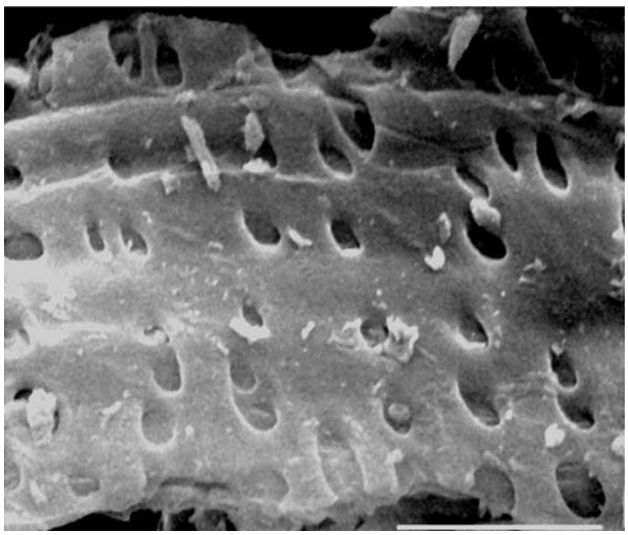

Fig. 25 SEM image of TSCC after treatment of As(III) in column operation

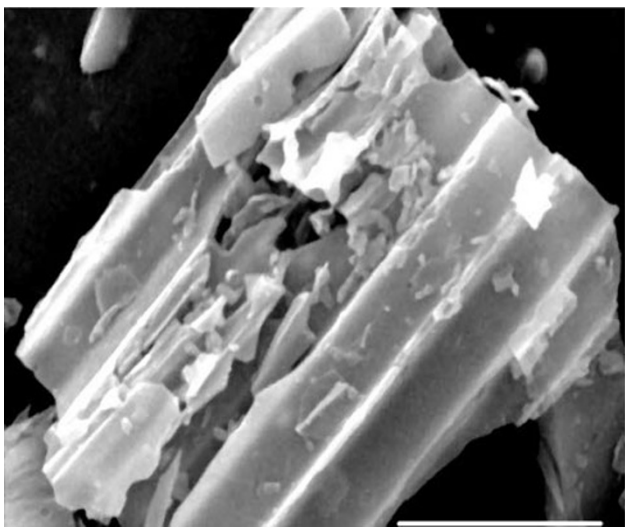

Fig. 26 SEM image of TSCC after treatment of As(V) in batch operation

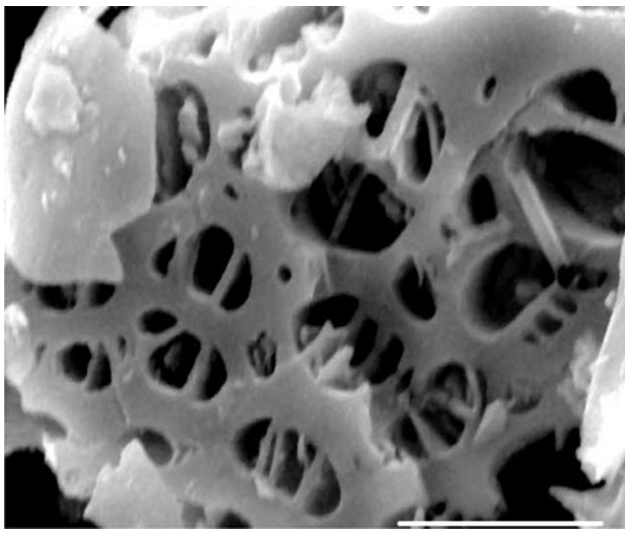

Fig. 27 SEM image of TSCC after treatment of As(V) in column operation

asymmetrical stretching, C=O stretching of saturated acid, skeletal vibration of aromatic C=C, deformational vibration of =C–H of alkenes, and –C–H out of plane deformation of aromatic compounds, respectively. A close examination of the spectra (Fig. 28) reveals a slight shift of the C–S axial stretching band from 1,094 cm^{-1} (Fig. 4) to 1,107 and 1,119 cm^{-1} also assigned to the same absorption peak. The FTIR spectrum of the adsorbent (TSCC) after treatment of As(III) shows three significant peaks at 1,718, 1,408 and 622 cm^{-1}. The 1,718 and 622 cm^{-1} peaks represent C=O stretching of saturated acid (Furniss et al. 2005; Ghosh 2006) and C–S stretching of thiol (Ghosh 2006), respectively, whereas 1,408 cm^{-1} reveals a slight shift of the deformational vibration of the =C–H band of alkenes from 1,420 cm^{-1}. Moreover, the presence of the characteristic frequency at 1,718 cm^{-1} and the newly appeared peak at 622 cm^{-1} reflect the probable mechanism of As(III) binding with the sulfur atom, whereas in case of As(V), the disappearance of the C=O stretching frequency of saturated acid also shows that As(V) binds with carboxylate groups (Fig. 13).

Comparison of adsorption capacity of TSCC with other adsorbents for the removal of arsenic

A literature review shows that only a few works on column studies have been reported, otherwise most of the studies for arsenic removal have been conducted in batch operation. However, the data obtained under batch conditions are generally not applicable in industrial and household treatment systems (such as column operations) where contact time is not sufficiently long for the attainment of equilibrium. Hence, there is a need to perform equilibrium studies using columns. The higher equilibrium uptake capacity in fixed bed column reactors, for the removal of both As(III) and As(V), makes the adsorbent attractive for arsenic removal filter units. Therefore, the uptake capacity in column operation on TSCC for As(III) and As(V) are compared with other adsorbents (Table 3). Although it is difficult to compare the TSCC directly with other low-cost adsorbents because of different applied experimental conditions, still it is found (Table 3) that the uptake capacity for arsenic adsorption on the TSCC is quite significant and is comparable to that of other adsorbents used for the removal of As(III) and As(V) in column mode. The results show the applicability of TSCC for the removal of As(III) and As(V) from aqueous solutions using an up-flow fixed bed continuous column.

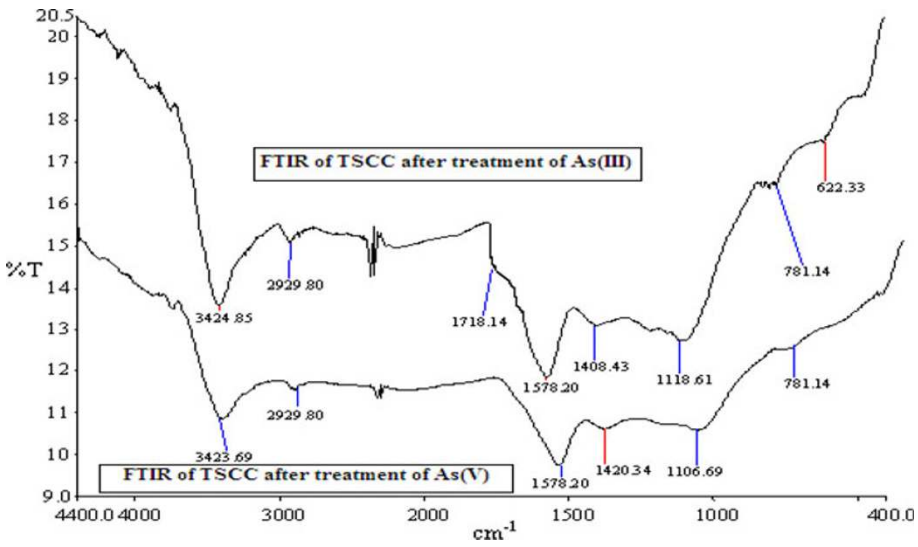

Fig. 28 FTIR spectra of TSCC after treatment of arsenic [As(III) and As(V)]

Table 3 Comparison of adsorption capacities of different adsorbents for the removal of arsenic by column operation

	Adsorbent	Conditions	Adsorption capacity (mg g^{-1})		References
			As(III)	As(V)	
1.	Waste rice husk	Rice husk, 6 g; concn, 100 μg mL^{-1}; pH 6.5; flow rate, 6.7 mL min^{-1}; av particle size, 780 μm	0.02		Amin et al. (2006)
		Rice husk, 6 g; concn, 100 μg mL^{-1}; pH 6.0; flow rate, 1.7 mL min^{-1}; av particle size, 510 μm		0.007	
2.	Activated alumina (AA)	Bed height, 6 cm; pH 7.6; flow rate, 0.016 cm^3 s^{-1}; av particle size, 0.2 ± 0.02 mm	0.384		Singh and Pant (2006)
3.	Iron oxide impregnated activated alumina (IOIAA)	Bed height, 6 cm; pH 12; flow rate, 0.016 cm^3 s^{-1}; av particle size, 0.2 ± 0.02 mm	0.460		
4.	Non-immobilized sorghum biomass (NISB)	NISB, 150 g; concn, 5 mg L^{-1}; pH 5.0; flow rate, 10 mL min^{-1}; av particle size, 0.18–1.4 mm	2.765 mg of As g^{-1}		Haque et al. (2007)
5.	Immobilized sorghum biomass (ISB)	ISB, 140 g; concn, 5 mg L^{-1}; pH 5.0; flow rate, 10 mL min^{-1}; av particle size, 0.25–0.5 mm	2.437 mg of As g^{-1}		
6.	Modified calcined bauxite (MCB)	Temp, 27 ± 2 °C; bed height, 10 cm; concn, 1 mg L^{-1}; pH 6.8 ± 0.4; flow rate, 5 mL min^{-1}; av particle size, 0.212 mm	0.490		Bhakat et al. (2007)
7.	Siderite coated sand (SCS) prepared by homogeneously mixing 0.04–0.08 mm siderite with 1.0 % HNO_3 rinsed 0.10–0.25 mm quartz sand at a ratio of 1:5 in weight	Bed height, 150 mm; concn, 500 μg L^{-1}; flow rate, 1.48 mL min^{-1}		1.09	Guo et al. (2007)
8.	Natural laterite (NA)	Temp, 27 ± 2 °C; bed height, 30 cm; pH 5.5 ± 0.1; concn, 1 mg L^{-1}; flow rate, 5 mL min^{-1}; av particle size, 0.273 mm		0.147	Maiti et al. (2008)
9.	Hydrous ferric oxide incorporated onto granular activated carbon with phenol formaldehyde resins coating (HFO-PF-coated GAC)	HFO-PF-Coated GAC, 1.5 g; concn, 1,470 μg L^{-1}; pH 6.8; flow rate, 1.57 mL min^{-1}		1.52	Zhuang et al. (2008)
10.	Ferrosorp plus (FP)	Temp, 21 ± 2 °C; FP, 120 g; concn, 2.8 μM; pH 6.8; flow rate, 50 mL h^{-1}; av particle size, 0.6–1.0 mm	10.57 μmol g^{-1}		Fuhrman et al. (2008)
11.	Rice polish	Temp, 30 °C; rice polish, 30.5 g; concn, 1,000 μg L^{-1}; pH 7.0; flow rate, 1.66 mL min^{-1}; av particle size, <178 μm	0.067		Ranjan et al. (2009)
		Temp, 30 °C; rice polish, 30.5 g; concn, 1,000 μg L^{-1}; pH 4.0; flow rate, 1.66 mL min^{-1}; av particle size, <178 μm		0.079	
12.	Hybrid resin prepared by combination of a polymeric anion exchange resin and an iron oxide with a goethite structure (Lewatit FO 36)	Lewatit FO36, 2.45 g; concn, 0.5 mg L^{-1}; pH 7.5; flow rate, 8 mL min^{-1}; av particle size, 0.35 mm		3.229	Boldaji et al. (2010)
13.	Zr-type adsorbent synthesized by radiation-induced graft polymerization with a phosphoric monomer onto a nonwoven cotton fabric and with subsequent modification by Zr(IV) loading on phosphoric units	Bed height, 0.3 cm; concn, 1 mg L^{-1}; pH 2; flow rate, 200 h^{-1}		0.1 mmol g^{-1}	Hoshina et al. (2012)
14.	Calix [4] arene-appended functional material (DE-4 resin)	Bed height, 10 cm; concn, 30 μg L^{-1}; pH 4.0; flow rate, 2 mL min^{-1}	0.412		Qureshi and Memon (2012)
15.	Thioglycolated sugarcane carbon (TSCC)	Temp, 30 °C; TSCC, 6.0 g; concn, 1,500 μg L^{-1}; pH 6.0; flow rate, 3.0 mL min^{-1}; av particle size, 250 μm	0.085	0.084	Present study

Conclusions

A thioglycolic acid impregnation methodology was applied to prepare a cost-effective porous arsenic adsorbent (TSCC) from sugarcane carbon. The adsorption efficiency of TSCC for removal of arsenic [As(III) and As(V)] from contaminated waters was studied. Batch operations under different experimental conditions were conducted to investigate the ability of a material to adsorb as well as the adsorption capacity of the material. The maximum removal of As(III) and As(V) species on TSCC from arsenic spiked distilled water are found to be 92.7 and 91.4 %, respectively. The batch adsorption was evaluated by ANN model which showed the validity of TSCC as an effective adsorbent for arsenic [As(III) and As(V)] removal. Column operations, under different conditions, were also employed to study its practical applicability of TSCC in the removal of arsenic [As(III) and As(V)] species. The data were processed according to the Thomas model and the column performance could be predicted by this model with high correlation coefficient and very low SE. Examinations of SEM and FTIR spectroscopy studies show that high arsenic uptake favored a surface complexation mechanism on the adsorbent surface.

Acknowledgments The authors are thankful to Dr. Barin Kumar Ghosh, Professor in Chemistry, Department of Chemistry, University of Burdwan, West Bengal, India for providing active support in FTIR data analysis and also sincere thanks to Dr. Srikanta Chakraborty, in charge of SEM, USIC, University of Burdwan, West Bengal, India for providing spontaneous help and support during the SEM study.

References

Amin NK (2008) Removal of reactive dye from aqueous solutions by adsorption onto activated carbons prepared from sugarcane bagasse pith. Desalination 223:152–161. doi:10.1016/j.desal.2007.01.203

Amin MN, Kaneco S, Kitagawa T, Begum A, Katsumata H, Suzuki T, Ohta K (2006) Removal of arsenic in aqueous solutions by adsorption onto waste rice husk. Ind Eng Chem Res 45:8105–8110. doi:10.1021/ie060344j

Aringhieri R, Pardini G, Gispert M, Sole A (1992) Testing a simple methylene blue method for surface area estimation in soils. Agrochimica 36:224–232

Awual MR, Jyo A (2009) Rapid column-mode removal of arsenate from water by crosslinked poly(allylamine) resin. Water Res 43:1229–1236. doi:10.1016/j.watres.2008.12.018

Bhakat PB, Gupta AK, Ayoob S (2007) Feasibility analysis of As(III) removal in a continuous flow fixed bed system by modified calcined bauxite (MCB). J Hazard Mater B139:286–292. doi:10.1016/j.jhazmat.2006.06.037

Bhaumik R, Mondal NK, Das B, Roy P, Pal KC (2011) Predicting iron adsorption capacity and thermodynamics onto calcareous soil from aqueous solution by linear regression and neural network modeling. Universal J Environ Res Technol 1:486–499

Biterna M, Antonoglou L, Lazou E, Voutsa D (2010) Arsenite removal from waters by zero valent iron: batch and column tests. Chemosphere 78:7–12. doi:10.1016/j.chemosphere.2009.10.007

Boldaji MR, Nabizadeh R, Dehghani MH, Nadafi K, Mahvi AH (2010) Evaluating the performance of iron nanoparticle resin in removing arsenate from water. J Environ Sci Health Part A Toxic/Hazard Subst Environ Eng 45:946–950. doi:10.1080/10934521003772337

Chiavola A, D'Amato E, Baciocchi R (2012) Ion exchange treatment of groundwater contaminated by arsenic in the presence of sulphate. Breakthrough experiments and modeling. Water Air Soil Pollut 223:2373–2386. doi:10.1007/s11270-011-1031-2

Das B, Mondal NK (2011) Calcareous soil as a new adsorbent to remove lead from aqueous solution: equilibrium, kinetic and thermodynamic study. Universal J Environ Res Technol 1:515–530

De AK (2008) Environmental Chemistry. New Age International, New Delhi

Devi NL, Yadav IC, Shihua QI (2009) Recent status of arsenic contamination in groundwater of northeastern india—a review. Rep Opin 1:22–32

Fuhrman HG, Wu P, Zhou Y, Ledin A (2008) Removal of As, Cd, Cr, Cu, Ni and Zn from polluted water using an iron based sorbent. Desalination 226:357–370. doi:10.1016/j.desal.0000.00.000

Furniss BS, Hannaford AJ, Smith PWG, Tatchell AR (2005) Vogel's textbook of practical organic chemistry. Infrared correlation tables, 5th edn. Pearson Education (Singapore) Pvt. Ltd., Delhi, pp 1412–1422

Ghosh SK (2006) Advanced general organic chemistry—a modern approach. UV–Visible and IR spectroscopy, 2nd edn. New Central Book Agency, Kolkata, p 371

Giri AK, Patel RK, Mahapatra SS (2011) Artificial neural network (ANN) approach for modelling of arsenic (III) biosorption from aqueous solution by living cells of *Bacillus cereus* biomass. Chem Eng J 178:15–25. doi:10.1016/j.cej.2011.09.111

Gregus Z, Roos G, Geerlings P, Nemeti B (2009) Mechanism of thiol-supported arsenate reduction mediated by phosphorolytic-arsenolytic enzymes II. Enzymatic formation of arsenylated products susceptible for reduction to arsenite by thiols. Toxicol Sci 110:282–292. doi:10.1093/toxsci/kfp113

Guo H, Stuben D, Berner Z (2007) Adsorption of arsenic(III) and arsenic(V) from groundwater using natural siderite as the adsorbent. J Colloid Interface Sci 315:47–53. doi:10.1016/j.jcis.2007.06.035

Gupta KR (2008) Water crisis in India. Atlantic, New Delhi

Gupta A, Sankararamakrishnan N (2010) Column studies on the evaluation of novel spacer granules for the removal of arsenite and arsenate from contaminated water. Bioresour Technol 101:2173–2179. doi:10.1016/j.biortech.2009.11.027

Han R, Wang Y, Yu W, Zou W, Shi J, Liu H (2007) Biosorption of methylene blue from aqueous solution by rice husk in a fixed-bed column. J Hazard Mater 141:713–738. doi:10.1016/j.jhazmat.2006.07.031

Hao J, Han MJ, Wang C, Meng X (2009) Enhanced removal of arsenite from water by a mesoporous hybrid material—Thiol-functionalized silica coated activated alumina. Microporous Mesoporous Mater 124:1–7. doi:10.1016/j.micromeso.2009.03.021

Haque N, Morrison GM, Perrusquia G, Gutierrez M, Aguilera AF, Cano-Aguilera I, Gardea-Torresdey JL (2007) Characteristics of arsenic adsorption to sorghum biomass. J Hazard Mater 145:30–35. doi:10.1016/j.jhazmat.2006.10.080

Hoshina H, Takahashi M, Kasai N, Seko N (2012) Adsorbent for Arsenic(V) removal synthesized by radiation-induced graft polymerization onto nonwoven cotton fabric. Int J Org Chem 2:173–177. doi:10.4236/ijoc.2012.23026

Kanwal F, Rehman R, Mahmud T, Anwar J, Ilyas R (2012) Isothermal and thermodynamical modeling of Chromium (III) adsorption by composites of polyaniline with rice husk and saw dust. J Chil Chem Soc 57:1058–1063. doi:10.4067/S0717-97072012000100022

Kemp W (1996) Organic Spectroscopy. Infrared Spectroscopy, 3rd edn. ELBS with Macmillan, Hong Kong, China, pp 19–99

Krishnan KA, Sreejalekshmi KG, Baiju RS (2011) Nickel(II) adsorption onto biomass based activated carbon obtained from sugarcane bagasse pith. Bioresour Technol 102:10239–10247. doi:10.1016/j.biortech.2011.08.069

Kumari P, Sharma P, Srivastava S, Srivastava MM (2005) Arsenic removal from the aqueous system using plant biomass: a bioremedial approach. J Ind Microbiol Biotechnol 32:521–526. doi:10.1007/s10295-005-0042-7

Lewinsky AA (2007) Hazardous materials and wastewater: treatment, removal and analysis. Nova Science, New York

Maiti A, DasGupta S, Basu JK, De S (2008) Batch and column study: adsorption of arsenate using untreated laterite as adsorbent. Ind Eng Chem Res 47:1620–1629. doi:10.1021/ie070908z

Maji SK, Pal A, Pal T, Adak A (2007) Modeling and fixed bed column adsorption of As(V) on laterite soil. J Environ Sci Health Part A 42:1585–1593. doi:10.1080/10934520701517713

Malkoc E, Nuhoglu Y (2006) Removal of Ni(II) ions from aqueous solutions using waste of tea factory: adsorption on a fixed-bed column. J Hazard Mater B135:328–336. doi:10.1016/j.jhazmat.2005.11.070

Mohan D, Pittman CU Jr (2007) Arsenic removal from water/wastewater using adsorbents—a critical review. J Hazard Mater 142:1–53. doi:10.1016/j.jhazmat.2007.01.006

Mondal MK (2010) Removal of Pb(II) from aqueous solution by adsorption using activated tea waste. Korean J Chem Eng 27:144–151. doi:10.1007/s11814-009-0304-6

Mondal NK, Roy P, Das B, Datta JK (2011) Chronic arsenic toxicity and it's relation with nutritional status: a case study in Purabasthali-II, Burdwan, West Bengal, India. Int J Environ Sci 2:1103–1118. doi:10.6088/ijes.00202020067

Nag JK, Balaram V, Rubio R, Alberti J, Das AK (1996) Inorganic arsenic species in groundwater: a case study from Purbasthali (Burdwan), India. J Trace Elem Med Biol 10:20–24. doi:10.1016/S0946-672X(96)80004-6

Nidheesh PV, Gandhimathi R, Ramesh ST, Singh TSA (2012) Adsorption and desorption characteristics of crystal violet in bottom ash column. J Urban Environ Eng 6:18–29. doi:10.4090/juee.2012.v6n1.018029

Nollet H, Roels M, Lutgen P, Meeren PV, Verstraete W (2003) Removal of PCBs from wastewater using fly ash. Chemosphere 53:655–665. doi:10.1016/S0045-6535(03)00517-4

Okieimen FE, Okundaye JN (1989) Removal of cadmium and copper ions from aqueous solutions with Thiolated Maize (Zea mays) Cob Meal. Biol Wastes 30:225–230. doi:10.1016/0269-7483(89)90123-7

Onwu FK, Ogah SPI (2010) Studies on the effect of pH on the sorption of cadmium (II), nickel (II), lead (II) and chromium (VI) from aqueous solutions by African white star apple (Chrysophyllum albidium) shell. Afr J Biotechnol 9:7086–7093

Pan X, Wang J, Zhang D (2009) Sorption of cobalt to bone char: kinetics, competitive sorption and mechanism. Desalination 249:609–614. doi:10.1016/j.desal.2009.01.027

Papaleo RM, Hallen A, Sundqvist BUR, Farenzena L, Livi RP, de Araujo MA, Johnson RE (1996) Chemical damage in poly(phenylene sulphide) from fast ions: dependence on the primary-ion stopping power. Phys Rev B 53:2303–2313. doi:10.1103/PhysRevB.53.2303

Qureshi I, Memon S (2012) Synthesis and application of calixarene-based functional material for arsenic removal from water. Appl Water Sci 2:177–186. doi:10.1007/s13201-012-0035-4

Rajesh Kannan R, Rajasimman M, Rajamohan N, Sivaprakash B (2010) Equilibrium and kinetic studies on sorption of malachite green using hydrilla Verticillata biomass. Int J Environ Res 4:817–824

Ranjan D, Talat M, Hasan SH (2009) Rice polish: an alternative to conventional adsorbents for treating arsenic bearing water by up-flow column method. Ind Eng Chem Res 48:10180–10185. doi:10.1021/ie900877p

Santamarina JC, Klein KA, Wang YH, Pencke E (2002) Specific surface: determination and relevance. Can Geotech J 39:233–241. doi:10.1139/T01-077

Sarkar S, Blaney LM, Gupta A, Ghosh D, SenGupta AK (2008) Arsenic removal from groundwater and its safe containment in a rural environment: validation of a sustainable approach. Environ Sci Technol 42:4268–4273. doi:10.1021/es702556t

Schmidt GT, Vlasova N, Zuzaan D, Kersten M, Daus B (2008) Adsorption mechanism of arsenate by zirconyl-functionalized activated carbon. J Colloid Interface Sci 317:228–234. doi:10.1016/j.jcis.2007.09.012

Sekhula MM, Okonkwo JO, Zvinowanda CM, Agyei NN, Chaudhary AJ (2012) Fixed bed column adsorption of Cu (II) onto Maize Tassel-PVA Beads. J Chem Eng Process Technol 3:1–5. doi:10.4172/2157-7048.1000131

Singh TS, Pant KK (2006) Experimental and modelling studies on fixed bed adsorption of As(III) ions from aqueous solution. Sep Pur Technol 48:288–296. doi:10.1016/j.seppur.2005.07.035

Skinner MF, Zabowski D, Harrison R, Lowe A, Xue D (2001) Measuring the cation exchange capacity of forest soils. Commun Soil Sci Plant Anal 32:1751–1764. doi:10.1081/CSS-120000247

Srivastava S, Raj KR, Kardam A (2012) Efficient arsenic depollution in water using modified maize powder. Environ Chem Lett. doi:10.1007/s10311-012-0376-0

Suresh S, Srivastava VC, Mishra IM (2012) Adsorptive removal of aniline by granular activated carbon from aqueous solutions with catechol and resorcinol. Environ Technol 33:773–781. doi:10(1080/09593330)2011592228

Teixeira MC, Ciminelli VST (2005) Development of a biosorbent for Arsenite: structural modeling based on X-ray spectroscopy. Environ Sci Technol 39:895–900. doi:10.1021/es049513m

Thomas HC (1944) Heterogeneous ion exchange in a flowing system. J Am Chem Soc 66:1664–1666. doi:10.1021/ja01238a017

Tiwari A, Dewangana T, Bajpai AK (2008) Removal of toxic As (V) ions by adsorption onto alginate and carboxymethyl cellulose beads. J Chin Chem Soc 55:952–961

Wasiuddin NM, Tango M, Islam MR (2002) A novel method for arsenic removal at low concentrations. Energy Sources Part A 24:1031–1041. doi:10.1080/00908310290086914

Yang L, Wu S, Paul CJ (2007) Modification of activated carbon by polyaniline for enhanced adsorption of aqueous arsenate. Ind Eng Chem Res 46:2133–2140. doi:10.1021/ie0611352

Zhuang JM, Hobenshield E, Walsh T (2008) Arsenate sorption by hydrous ferric oxide incorporated onto granular activated carbon with phenol formaldehyde resins coating. Environ Technol 29:401–411. doi:10.1080/09593330801984399